Accepted Manuscript

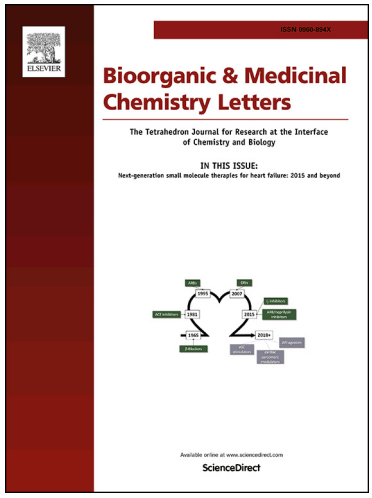

Lead generation of 1,2-dithiolanes as exon 19 and exon 21 mutant EGFR tyrosine kinase inhibitors

Tarek S. Mansour, Vijay Potluri, Ranga R. Pallepati, Vishnu Basetti, Mallaiah Keesara, Ashok G. Moghudula, Pranab Maiti

PII: S0960-894X(19)30251-3
DOI: https://doi.org/10.1016/j.bmcl.2019.04.029
Reference: BMCL 26396

To appear in: *Bioorganic & Medicinal Chemistry Letters*

Received Date: 15 February 2019
Revised Date: 15 April 2019
Accepted Date: 18 April 2019

Please cite this article as: Mansour, T.S., Potluri, V., Pallepati, R.R., Basetti, V., Keesara, M., Moghudula, A.G., Maiti, P., Lead generation of 1,2-dithiolanes as exon 19 and exon 21 mutant EGFR tyrosine kinase inhibitors, *Bioorganic & Medicinal Chemistry Letters* (2019), doi: https://doi.org/10.1016/j.bmcl.2019.04.029

Lead generation of 1,2-dithiolanes as exon 19 and exon 21 mutant EGFR tyrosine kinase inhibitors

Tarek S. Mansour [a], Vijay Potluri [b], Ranga R. Pallepati [b], Vishnu Basetti [b], Mallaiah Keesara [b], Ashok G. Moghudula [b], Pranab Maiti [b]

[a] Sabila Biosciences LLC, 5 Overlook Road, New City, New York 10956 U.S.A.

[b] Aurigene Discovery Technology Ltd. Bollaram Road, Miyapur, Hyderabad, 500 049, Telangana India

Corresponding author: tsmansour@sabilabiosciences.com

Non-small cell lung cancer (NSCLC) is the most common type (80-85%) of lung cancer sub-categorized into adenocarcinoma, squamous cell carcinoma and large cell carcinoma. Unfortunately, the majority of NSCLC cases are diagnosed in patients reaching localized advanced stage III or metastatic stage IV and thus require some form of chemotherapy intervention. Over 160,000 deaths occurred in the USA in 2018 due to respiratory system cancers including NSCLC.[1] Initial therapy with the first-generation tyrosine kinase inhibitors (TKIs) erlotinib, gefitinib and icotinib achieved remarkable benefits targeting the endothelial growth factor receptor (EGFR) tyrosine kinase domain. Mutations in EGFR which activate the RAS signaling pathway, occur to the extent of 85% in NSCLC due to exon 19 deletions (E746-A750del, ex19del) and exon 21 point mutations such as (L858R). Gefitinib was first approved for primary NSCLC that contains activating mutations $EGFR^{L858R/ex19del}$. Second-generation TKIs such as neratinib, canertinib, dacomitinib and afatinib were designed to covalently target a conservative Cys797 residue in both wild type (WT) and mutant EGFR thus enhancing their kinome selectivity and duration of response due to longer target engagement in the presence of high intracellular concentrations of ATP. However, rapid emergence of resistance to all clinically used first and second-generation TKIs in about 50% of patients, limits their clinical benefit due to selection of a single gatekeeper mutation T790M (exon 20) that increases affinity to ATP and restricts access to a hydrophobic binding pocket. To overcome acquired resistance to $EGFR^{T790M}$, third-generation covalent TKIs,[2-4] osimertinib and olmutinib were developed[3] and a number of experimental drugs such as nazartinib,[5] naquotinib,[6] avitinib,[7] PF06747775[8] and others are in various stages of development.[9,10] Despite these impressive advances, multiple resistance mechanisms to osimertinib and olmutinib have been reported most notably dominated by the emergence of a C797S mutation in about 40% of clinical cases.[2-4] Ironically, this mutation prevents the formation of a covalent bond between the inhibitors and Cys797. The intense clinical and regulatory activities in the period of 2013-2018 resulted in the FDA approval of erlotinib, gefitinib, afatinib, osimertinib and olmutinib covering different modalities to treat NSCLC patients. Current research efforts have focused on further development of fourth-generation inhibitors with a profile of inhibiting, activating mutations (L858R, exon19del), T790M and the C797S mutations ($EGFR^{L858R/T790M/C797S}$) and indeed, good progress has been made as in brigatinib[11]

(phase 2), the non-ATP allosteric inhibitor EA1045[12] and others,[3,13,14] although it remains to be seen whether these fourth-generation inhibitors will rapidly select for resistance as well.

An alternative strategy to developing fourth-generation inhibitors is based on combining $EGFR^{L858R/exdel19}$ first-generation and $EGFR^{T790M}$ third-generation inhibitors. The principle behind this strategy is supported by examining the allelic context of $EGFR^{C797S}$ and $EGFR^{T790M}$ selected by a combination of osimertinib with erlotinib which determines the sensitivity to the TKIs combination. Trans alleles (on the same clones) are sensitive to first and third-generation TKIs combinations, whereas cis alleles (different clones) are less effected.[15,16] Structural analysis suggests that the third-generation TKIs restore the cytoplasmic juxtamembrane segment structure to the conformation of EGFR in the wild-type state when activated by its natural ligand EGF.[17] This juxtamembrane segment structure which links the kinase domain with the extracellular regions is likely an important player since mutant and $EGFR^{WT}$ have similar kinase domains. We therefore, considered a strategy to address the rapid resistance to third-generation inhibitors by a *de novo* design of $EGFR^{L858R/exdel19}$ inhibitors for combination therapy with third-generation inhibitors. In this paper, we report on our lead identification efforts which led to novel $EGFR^{L858R/ex19del}$ TKIs that carry 1,2-dithiolanes as a possible moiety that might be targeted by the conservative Cys797 residue in an alternative fashion to acrylamide containing inhibitors. Sparing $EGFR^{WT}$ activity remains a desirable property of TKIs to limit skin rash side effects due to keratinocytes injury which eventually leads to release of IL-31, a known pruritus-inducing cytokine.[18]

Quinazolines and 3-cyanoquinolines were chosen as core heterocycles due to their precedents as EGFR inhibitors. Various *N*-4 headpiece moieties explored in this study (Figure 1) were selected from those in clinical candidates pelitinib/afatinib/canertinib/sapitinib/dacomitinib, lapatinib and CP-724,714. The key intermediates: 6-aminoquinazolines and -3-cyanoquinolines (Figure 1, **1-8**) were prepared by a displacement reaction of the 4-chloro heterocycles with anilines as previously described for **6**.[19]

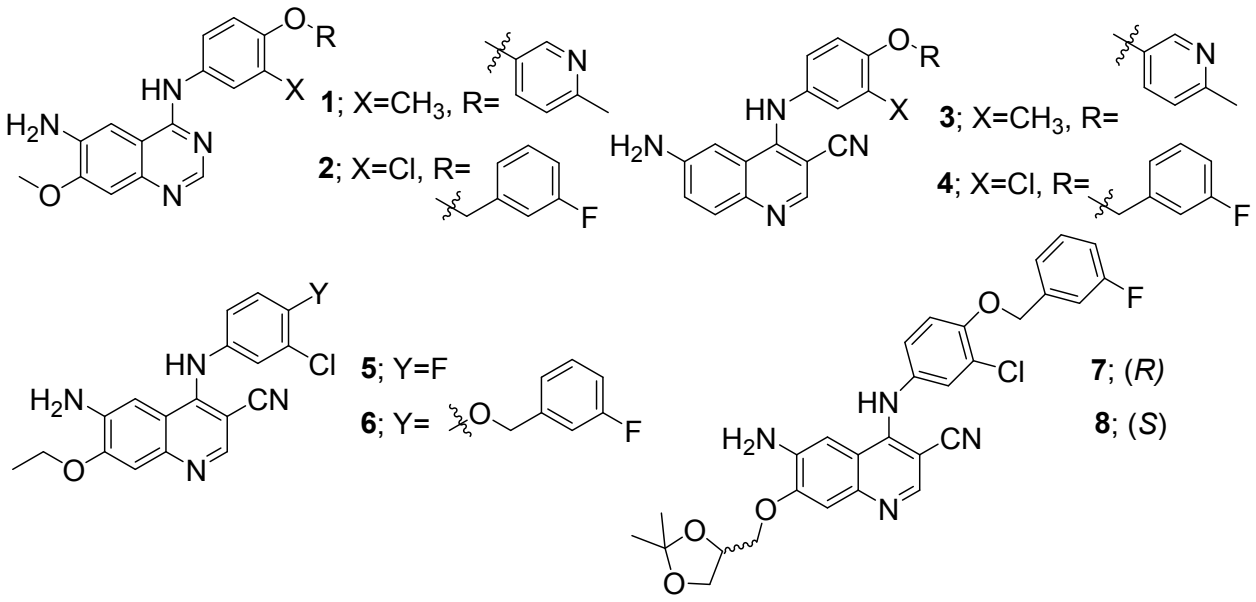

Figure 1. Key Aniline Intermediates **1-8**.

3-Cyanoquinolines **7** and **8** were prepared in 4 steps involving: 1) dealkylation of the 7-methoxy heterocycle **9** with BBr_3 in dichloromethane, 2) displacement of the 4-chloro moiety in **10** with 3-chloro-4-((3-fluorobenzyl)oxy)aniline, 3) *O*-alkylation of **11** using either (*S*) or (*R*)-(2,2-dimethyl-1,3-dioxolan-4-yl)methyl methanesulfonate with Cs_2CO_3 with *N*.*N*-dimethyl formamide , 4) hydrolysis with potassium hydroxide in methanol as shown in Scheme 1.

Scheme 1. Synthesis Protocol for 7 and 8

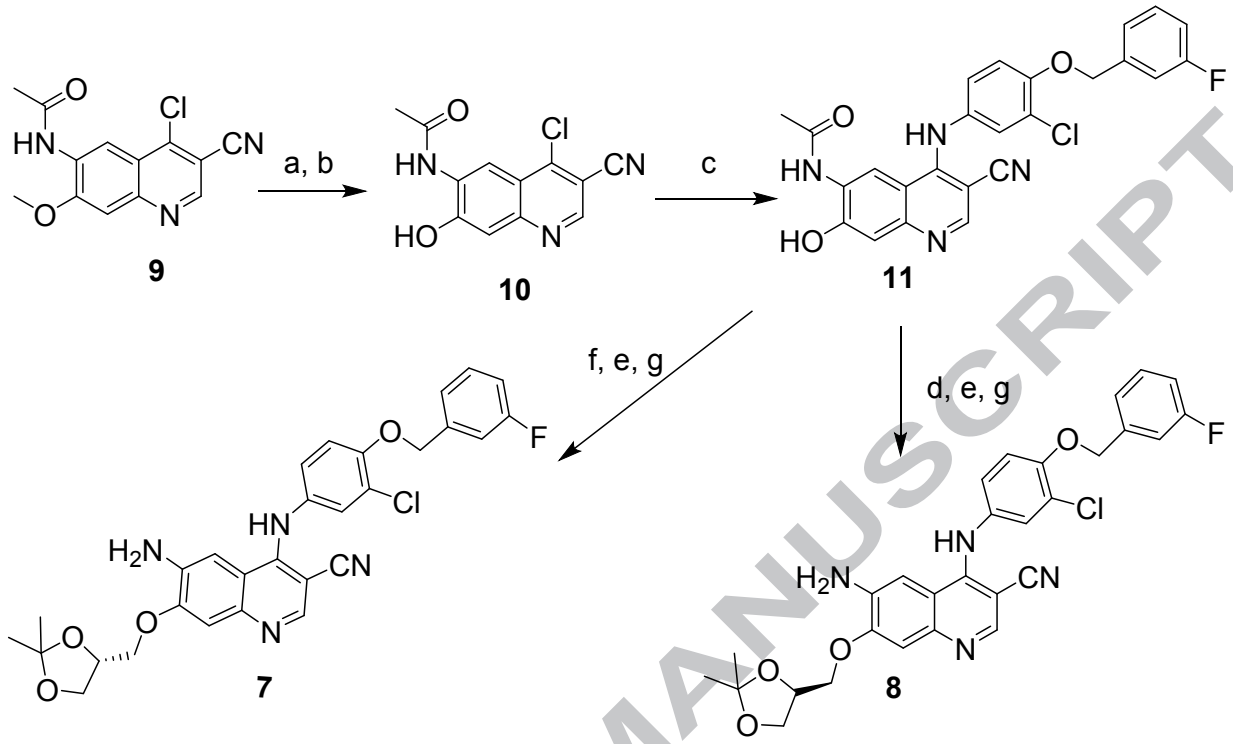

Reagents and conditions: (a) BBr_3 DCM, 0 ^oC 0.5 h, (b) 100 ^oC, 5 h, 80% , (c) 3-chloro-4-((3-fluorobenzyl)oxy) aniline, i-propanol, 150 ^oC 12 h 56%, (d) Cs_2CO_3 DMF, rt 0.5 , (e) (R)-(2,2-dimethyl-1,3-dioxolan-4-yl)methyl methanesulfonate 90 ^oC, 12 h, 12%, (f) (S)-(2,2-dimethyl-1,3-dioxolan-4-yl)methyl methanesulfonate 90 ^oC, 12 h, 12%, (g) KOH/MeOH 70 ^oC 6 h, 25%

Anilines **1-6** were coupled with various dithio derivatives using one of three methods A, B or C to furnish target compounds **13** – **32** (Schemes 2, 3). A direct coupling protocol of anilines **1**, **2**, **4**, and **6** with a 1,2 dithiolane acyl chloride generated *in situ* from 2-(1,2-dithiolan-3-yl)acetic acid **33** or lipoic acid **34** and oxalyl chloride in dichloromethane-tetrahydrofuran solvent system was achieved in method A. In this fashion, target compounds **16**, **17**, **19** and **22** were prepared.

In method B, a coupling agent such as 1-(3-dimethylaminopropyl)-3-ethylcarbodiimide hydrochloride (EDC) in *N*-methyl pyrrolidone was used to effect the reaction of anilines **3**, **5, 6** with asparagusic acid **35** as well as **33** and **34.** Method B proved to be useful for the preparation of **13**, **15**, **21**, **25** and **28**. In an alternative approach depicted as method C, 2-(bromomethyl)acrylic acid **36** was converted stepwise to 3-(acetylthio)-2-((acetylthio)methyl)propanoic acid **38** by reaction with thioacetic acid via the intermediacy of **37.** Compound **38** was then converted to its chloroacyl derivative S,S'-(2-(chlorocarbonyl)propane-1,3-diyl) diethanethioate **39** by reaction with oxalyl chloride. Coupling of **39** with anilines **1, 2, 3, 5** and **6** produced the corresponding S,S'-

carbamoyl)propane-1,3-diyl)diethanethioates which were isolated and treated with methanolic ammonia to provide compounds **14, 18, 20, 24,** and **27**. Conversion of **23** and **26** to **24** and **27** respectively was also achieved via hydrolysis of **23** and **26** with sodium borohydride in dimethyl acetamide followed by acid quench to produce bis-mercapto intermediates which were readily oxidized by dimethyl sulfoxide to asparagusic analogs **24** and **27**.

Scheme 2. Synthesis of TKIs by Methods A, B and C

Method A

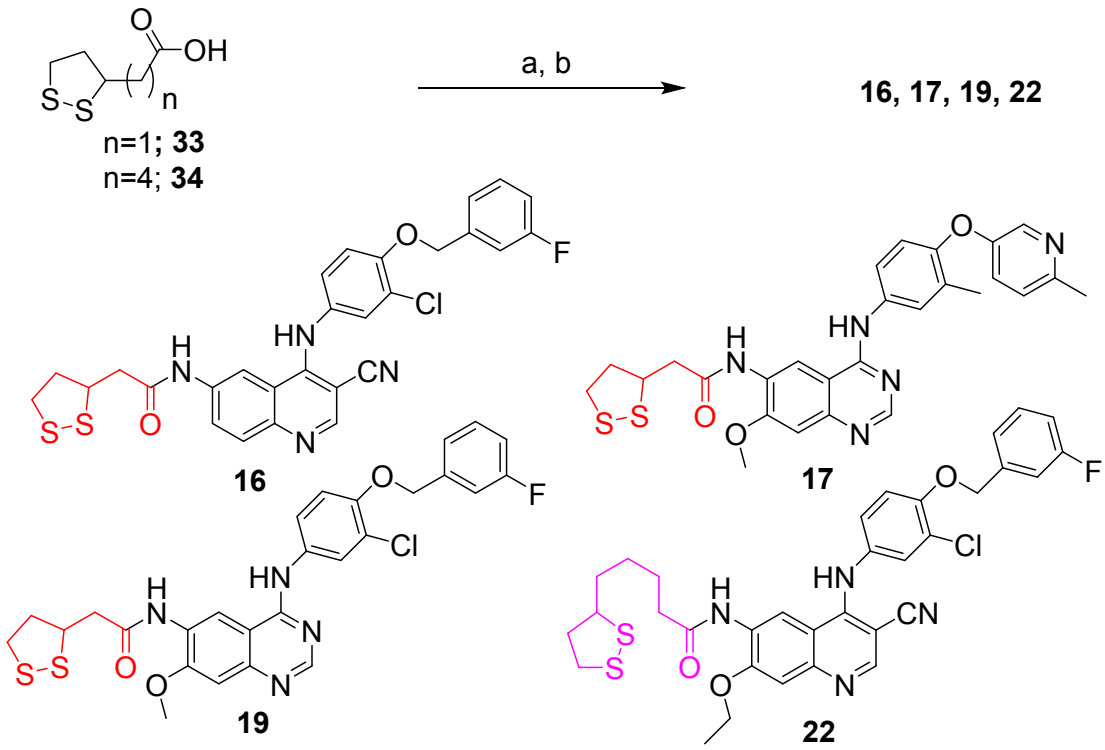

Reagents and conditions: (a) Oxalyl chloride, DCM-THF 0 °C, 15 min, (b) Anilines **1, 2, 4, 6,** DIEA, DMF-THF 0 °C, 1 h, 8-13% 2 steps.

Method B

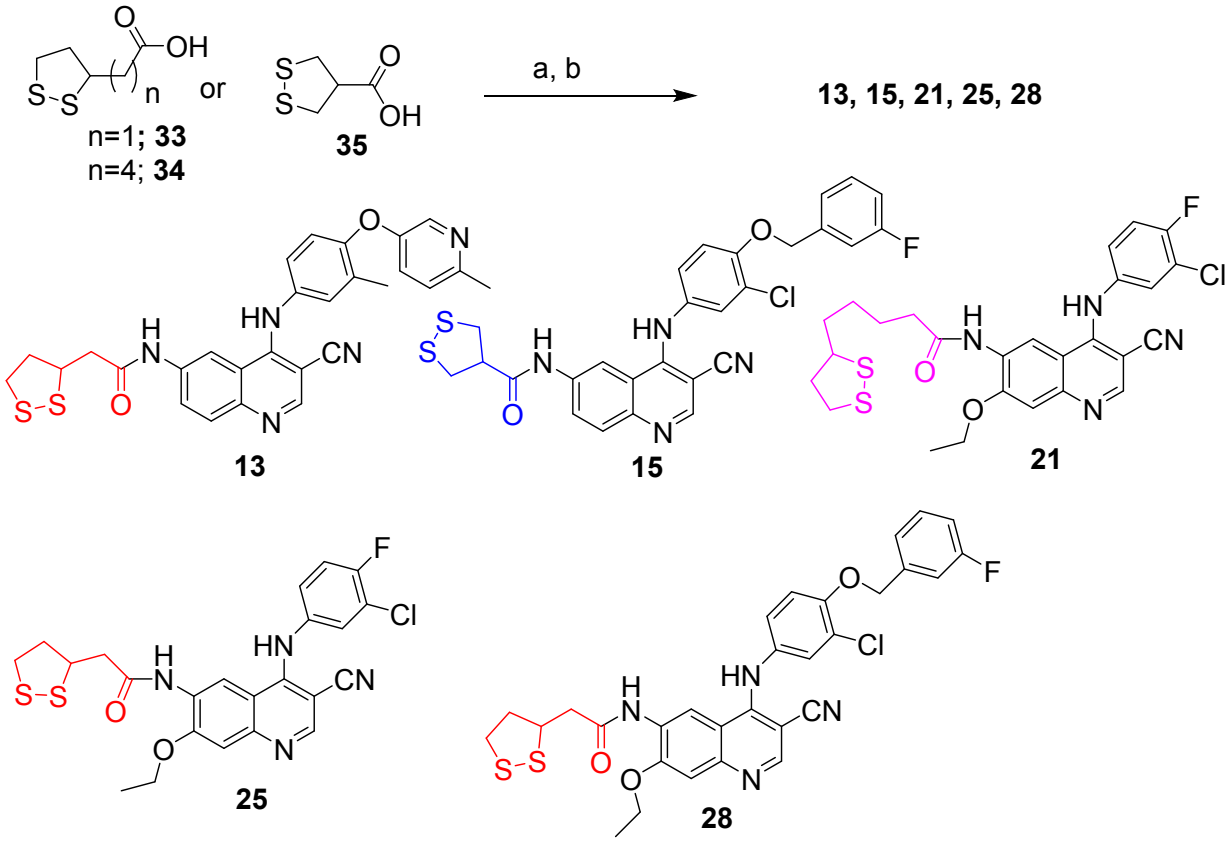

Reagents and Conditions: (a) EDC, NMP (b) Anilines **3, 5, 6** rt 2 h, 17-37% 2 steps

Method C

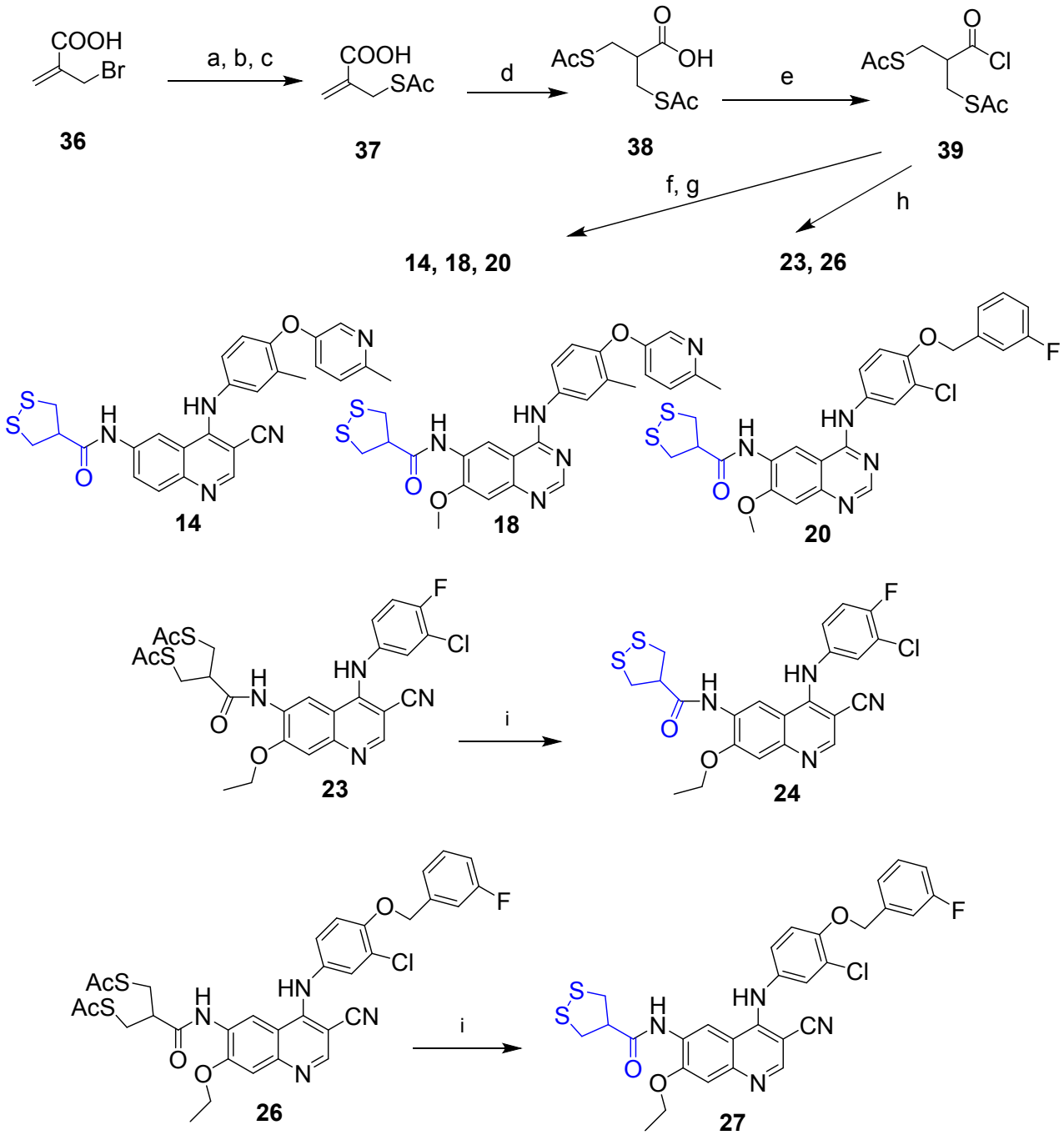

Reagents and conditions: (a) Na_2CO_3-H_2O 47% (b) AcSH (c) HCl 45% (d) AcSH 45% (e) Oxalyl chloride DCM-THF, DIEA 0 ^oC, 1 h, (f) anilines **1, 2, 3** (g) NH_3 in MeOH 2-4% 3 steps from **38** (h) anilines **5**, **6** 4% (i) **23** to **24** and **26** to **27** $NaBH_4$ DMA (i) DMSO 120 ^oC, 1 h, 12-17% 2 steps

Compounds **29**-**32** were prepared following the protocols in method C (Scheme 3) by coupling of **7** and **8** with **38** to produce **39** and **40** respectively, followed by deprotecting of acetonides with acid to diols **29** and **30**. Oxidative hydrolysis to 1,2 dithiolanes **31** and **32** was achieved by methanolic ammonia in dichloromethane.

Scheme 3. Synthesis of 29-32

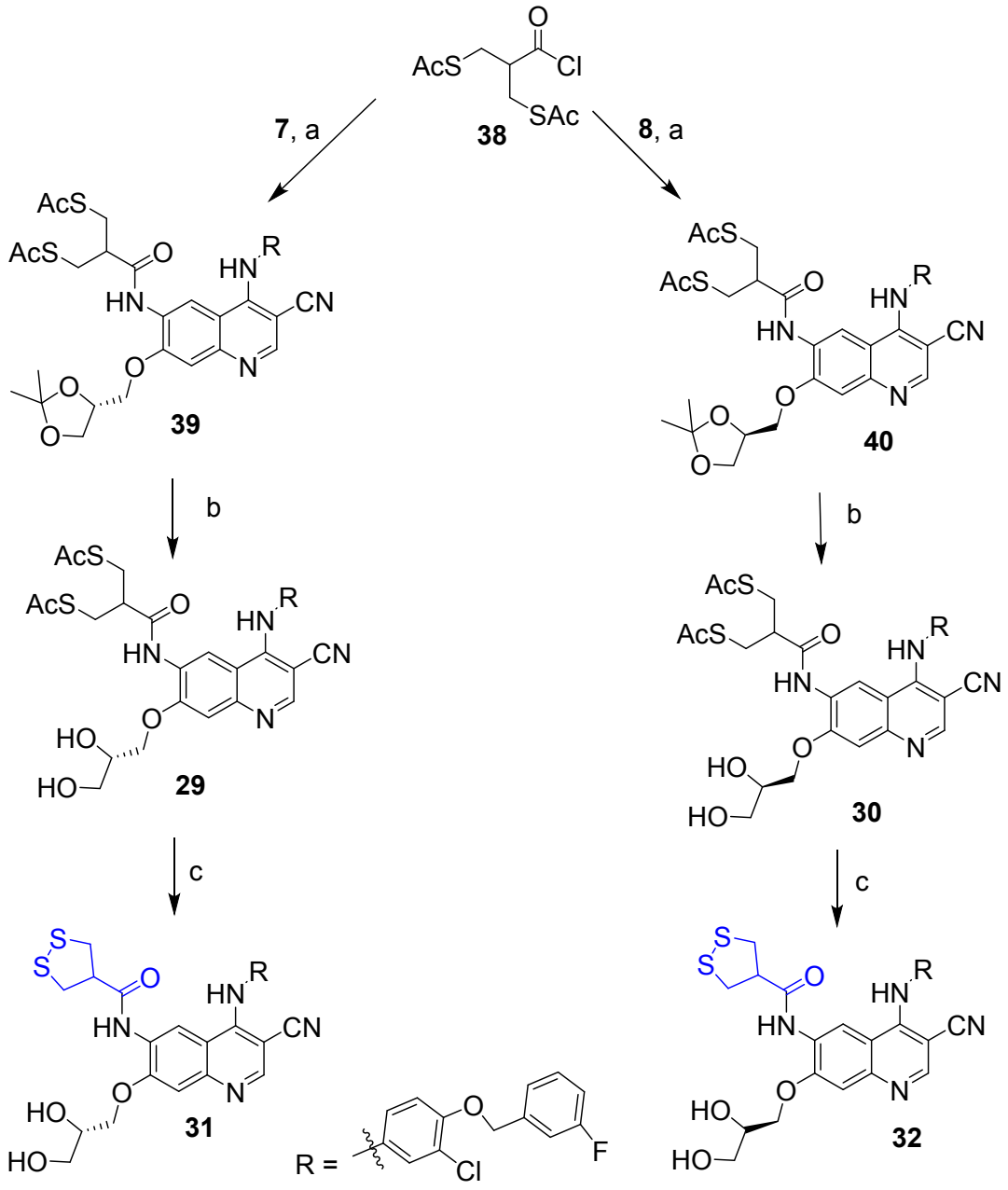

Reagents and conditions: (a) Method C DIPEA-DCM, rt 2 h, 34-63% (b) HCl MeOH rt 30 min, 10% (c) NH_3 MeOH rt 30 min, 75%

The SAR was assessed in two biochemical binding assays: rabbit reticulocyte lysate and KINOME*scan*™. Initially, inhibitors **13**-**32** were evaluated against $EGFR^{WT}$ and $EGFR^{L858R}$ and Her2 kinases in the rabbit reticulocyte lysate assay (*Kinase*Seeker™) which contains the cellular components necessary for protein synthesis. This assay is a homogeneous competition binding assay where the displacement of an active site dependent probe by an inhibitor is measured by a change in luminescence signal reported in IC_{50} values.[20] Luminescence readout translates into a highly sensitive and robust assay with low background and minimal interference from test compounds.

The activity of compounds in mutant EGFR was assessed in the KINOME*scan*™ assay which is a competition binding assay that quantitatively measures the ability of a compound to compete with an immobilized, active-site directed ligand. The ability of the test compound to compete with the immobilized ligand is measured via quantitative PCR of the DNA tag and reported as inhibitor binding constants (Kd values) from duplicate 11-point dose response curves.[21]

In the set of 3-cyanoquinolines (**13**-**16**) lacking any C7 substituent, **13** and **14** displayed weaker activity against $EGFR^{WT}$ and $EGFR^{L858R}$ than **15** and **16** suggesting that the 3-chloro-4-((3-fluorobenzyl)oxy)anilino headpiece is preferred over the 3-methyl-4-((6-methylpyridin-3-yl)oxy)anilino moiety of **13** and **14**. This finding was consistently observed in the 7-methoxyquinazolines **17**-**20** where **19** and **20** emerged 8-60 fold more potent than **17** and **18** against $EGFR^{L858R}$. Preference for inhibiting $EGFR^{L858R}$ by inhibitors containing the 3-chloro-4-((3-fluorobenzyl)oxy)anilino over 3-chloro-4-fluoroanilino headpieces was established in several pairs of lipoic acid conjugates **21** and **22**, asparagusic acid conjugates **24** and **27** and, 2-(1,2-dithiolan-3-yl)acetic acid conjugates **25** and **28.** From this set of inhibitors, we deduced that asparagusic and 2-(1,2-dithiolan-3-yl)acetic acid conjugates have similar activity against $EGFR^{L858R}$ and both conjugates displayed good selectivity over $EGFR^{WT}$. Acyclic intermediates **23** and **26** were about 2-fold less active against $EGFR^{L858R}$ than target compounds **24** and **27** respectively. The 7-dihydroxypropyl analogs **31** and **32** maintained the increased inhibition of $EGFR^{L858R}$ with good selectivity over $EGFR^{WT}$ (Table 1). In this pair, small preference for the *S* stereochemistry was noted. Compounds **15, 21, 23-25** were not evaluated against $EGFR^{WT}$ due to their modest activity against $EGFR^{L858R}$.

Table 1. SAR in Rabbit Reticulocyte Assay (IC_{50} Values in nM)*

Entry	Compound	$EGFR^{WT}$	$EGFR^{L858R}$	Method
1	**13**	8630 ± 850	>10,000	B
2	**14**	>10,000	>10,000	C
3	**15**	NT	199 ± 19	B
4	**16**	164 ± 15	36 ± 12	A
5	**17**	253 ± 20	48 ± 8	A
6	**18**	658 ± 219	413 ± 68	C
7	**19**	25 ± 2	5.8 ±1	A
8	**20**	76 ± 6	6.5 ± 0.8	C
9	**21**	NT	420 ± 5	B
10	**22**	730 ± 65	33 ± 4	A
11	**23**	NT	494 ± 30	C
12	**24**	NT	219 ± 47	C
13	**25**	NT	300 ± 40	B
14	**26**	340 ± 67	26.8 ± 4.2	C
15	**27**	210 ± 20	18 ± 3	C
16	**28**	120 ± 19	10.9 ± 1.9	B
17	**31**	125 ± 12	9 ± 2	C
18	**32**	256 ± 21	20 ± 7	C

*Ten point dose response curve, each value is an average of triplicate experiments

It was deemed of relevance to benchmark the inhibitors against a select set of clinical and marketed compounds including mutant selective as well as first-generation inhibitors. Since historical data in the rabbit reticulocyte assay were limited for these inhibitors, the IC_{50} values (in nM) were determined in this assay format (Supplementary Figure 1). Inhibitor **28** compared well to this set and was considered worthy of further evaluation.

In order to determine the activity of lead candidates in mutant EGFR enzymes other than $EGFR^{L858R}$, the KINOME*scan*™ assay was chosen because it had the ability to test all relevant mutants of EGFR. Thus, we first established the correlation between the rabbit reticulocyte and KINOME*scan*™ assays by comparing the IC_{50} and K_d values for three most potent inhibitors **22, 26** and **28** against $EGFR^{L858R}$. The data (Supplementary Table 1) showed excellent correlation between the two assay formats thus justifying the use of this assay to determine the activity in mutant EGFR.

Next, the activity of lead candidate **28** was determined against several activating EGFR mutations including the highly frequent deletion mutation of $EGFR^{ex19del}$. The K_d values were in the range of 4.8-48 nM against ten EGFR variants including the $EGFR^{L861Q}$,

$EGFR^{G719C}$ and $EGFR^{ex19del}$ mutants (Supplementary Table 2). Inhibitor **28** displayed good activity (48 nM) against the $EGFR^{ex19del}$ mutant, being about 2-4 fold better in comparison to the asparagusic acid analog **27** (110 nM) which contains the isomeric 1,2-dithiolanyl moiety and its precursor **26** (180 nM) respectively.

To evaluate kinase selectivity, Her2 the closely related ErbB family member was chosen. In this case all $EGFR^{L858R}$ inhibitors tested displayed good selectivity (> 25 fold) over Her2 in the same rabbit reticulocyte lysate assay format with **17** being the least selective (Table 2). Moreover, **28** displayed even greater selectivity (Supplementary Table 3) over several TEC family kinases (TEC, BMX, BTK, and ITK).

Table 2. IC_{50}* Values (nM) against Her2

Entry	Compound	$EGFR^{WT}$	$EGFR^{L858R}$	Her2
1	**13**	8630 ± 850	>10,000	>10,000
2	**16**	164 ± 15	36 ± 12	730 ± 150
3	**17**	253 ± 20	48 ± 8	93 ± 19
4	**18**	658 ± 219	413 ± 68	590 ± 155
5	**27**	210 ± 20	18 ± 3	730 ± 150
6	**28**	120 ± 19	10.9 ± 1.9	160 ± 20
7	**31**	125 ± 12	9 ± 2	167 ± 20

*Ten point dose response curve, each value is an average of triplicate experiments

Prior to this letter, the kinome activity of 1,2 dithiolane carboxamides was rather limited.[22] Melchiorre *et al*,[23] proposed an intriguing multitarget-directed drug discovery strategy by combining structural features of oxidative stress and EGFR molecular recognition elements represented by **41** (Supplementary Figure 2) which contains a 6-substituted 1,2-dithiolanyl carboxamide with a quinazoline core. Based on reversibility data in human epidermoid carcinoma A431 cells which overexpress EGFR and molecular modeling studies, the investigators concluded that **41** irreversibly block EGFR by a thiol-disulfide interchange reaction involving Cys797 of EGFR and the disulfide moiety of **41**. We have utilized scanKINETIC™ assay to evaluate the association/dissociation kinetics of two inhibitors **31** and **30**. In this assay, the inhibitor binding kinetics are determined by measuring and comparing the K_d values under four sets of dose-response: 1) arm A: full equilibrating; 2) arm B: equilibrate/3-fold dilution/equilibrate; 3) arm C: partial equilibration and 4) arm D: predilution/full equilibration. The K_d values for **31** against $EGFR^{L858R}$ under these four conditions was determined to be 0.7, 8.4, 1.9 and 16 nM. This suggests that **31** kinetics are consistent with a reversible inhibitor with rapid dissociation kinetics (K_d arm B/ K_d arm A =12) and relatively slow association kinetics (K_d arm C/ K_d arm A =2.7). Furthermore, compound **30** which is an open chain analog of **31** had K_d values against $EGFR^{L858R}$ in the scanKINETIC™ assay as follows: 2.1, 58, 5.9 and 60 nM in arms A-D respectively. These data suggest that relative to **31**, compound **30** has even faster dissociation

kinetics but similar slow association kinetics (Supplementary Table 4). Therefore, on the basis of these findings, it was concluded that **30** and **31** do not bind $EGFR^{L858R}$ in an irreversible manner.[24] The apparent difference between our results and those of Melchiorre *et al* regarding the involvement of a possible thiol-disulfide interchange reaction may be due to the assay format (biochemical versus cellular), choice of dithiolane substrate with 4 versus 3-substituted dithiolanes, lack of C7 substituent or the nature of the kinase ($EGFR^{L858R}$ versus $EGFR^{WT}$).

Inhibitor **28** has acceptable CYP isoforms 1A2, 3A4, 2B6, 2C8, 2C9, 2C19, 2D6 and metabolic profiles in S9, liver microsomes and hepatocytes (Supplementary Tables 5 and 6). In the NCI-60 panel, **28** as well as **17** demonstrated good cellular activity relative to gefitinib against three NSCLC cell lines and two leukemia lines with GI_{50} values in the range of 0.11-1.07 μM (Table 3). The desirable high LC_{50} values obtained resulted in excellent therapeutic index (2->227) in this set of cell lines.

Table 3. Cellular Activity in μM of 17, 28 and Gefitinib in Select Cells in the NCI-60 Panel[a]

		17			**28**		**Gefitinib**
Cell Line	GI_{50}[b]	LC_{50}[c]	TI[d]	GI_{50}[b]	LC_{50}[c]	TI[d]	GI_{50}[e]
NSCLC							
A549	0.76	NT		0.54	3.4	6.2	7.94
NCI-H322M	1.07	> 50	> 46.7	0.60	> 25	> 41.5	0.08
NCI-H460	0.11	NT		0.47	1.95	4.1	6.31
Leukemia							
CCRF-CEM	0.22	> 50	> 227	0.15	> 25	> 166	5.01
MOLT-4	0.16	> 2.6	16.2	0.16	> 25	> 156	3.98

(a) Five dose response curve, each value is an average of 2 experiments; (b) GI_{50} is the concentration of the drug causing 50% growth inhibition (c) LC_{50} is the cytotoxic concentration due to 50% reduction in measured protein (d) LC_{50}/GI_{50} (e) data from the DTP-NCI database https://dtp.cancer.gov/services/nci60data/meangraph/gi50/jpg/-4.0/715055

In conclusion, we have outlined a new synthetic strategy to EGFR mutant selective inhibitors that led to the discovery of a new series of 1,2 dithiolane TKIs with potent activity against exon 19 deletion and exon 21 mutant EGFR. These inhibitors are selective over $EGFR^{WT}$, Her2 and TEC family kinases in the rabbit reticulocyte lysate assay. Two inhibitors **17** and **28** demonstrated good cellular activity and high therapeutic index in certain NSCLC and leukemia cell lines. Binding to $EGFR^{L858R}$ is shown to be reversible as determined by the scanKINETIC™ assay. The lead candidate **28** has good metabolic and excellent CYP isoform profile. Further optimization of lead candidate **28** shall be reported in due course.[24]

Acknowledgements: We thank the NCI DTP program (Bethesda, MD, USA) for cellular data, Reena Zutshi (Luceome Biotechnology, Tucson, AZ, USA)) and Jeremy Hunt (Eurofins, San Diego, CA, USA)) for all biochemical data, R Mamatha and S Kumar for CYP and metabolic stability data. We also thank Paul C. Anderson and Mahdi B. Fawzi for useful discussions on this research. This paper is dedicated with appreciation to Elie Abushanab (retired Professor) University of Rhode Island, RI, USA.

This research did not receive any specific grant from funding agencies in the public, commercial, or not-for-profit sectors

Declaration of interest: None

References and notes

1. Siegel RI, Miller KD, Jemal A. Cancer stats 2017. *CA Cancer. J Clin.* 2017;67:7-30.

2. Song, Z, Ge Y, Wang C, Huang S, Shu X, Liu K, Zhou Y, Ma X. Challenges and perspectives on the development of small-molecule EGFR inhibitors against T790M-mediated resistance in non-small-cell lung cancer. *J Med Chem.* 2016;59:6580–6594.

3. Chen L, Fu W, Zheng L, Liu Z, Liang G. Recent progress of small-molecule epidermal growth factor receptor (EGFR) inhibitors against C797S in non-small-cell lung cancer. *J Med Chem.* 2018;61:4290–4300.

4. Cheng H, Planken S. Precedence and promise of covalent inhibitors of EGFR and KRAS for patients with non-small-cell lung cancer. *ACS Med Chem Lett.* 2018:9:861-863.

5. Lelais G, Epple R, Marsilje TH, Long YO, McNeill M, Chen B, Lu W, Anumolu J, Badiger S, Bursulaya B, DiDonato M, Fong R, Juarez J, Li J, Manuia M, Mason DE, Gordon P, Groessl P, Johnson K, Jia Y, Kasibhatla S, Li C, Isbell J, Spraggon G, Bender S, Michellys PY. Discovery of (*R*,*E*)-*N*-(7-chloro-1-(1-[4-(dimethylamino)but-2-enoyl]azepan-3-yl)-1*H*-benzo[*d*]imidazol-2-yl)-2-methylisonicotinamide (EGF816), a novel, potent, and WT sparing covalent inhibitor of oncogenic (L858R, ex19del) and resistant (T790M) EGFR mutants for the treatment of EGFR mutant non-small-cell lung cancers. *J Med Chem.* 2016;59:6671–6689.

6. Wang S, Cang S, Lin D. Third-generation inhibitors targeting EGFR T790M mutation in advanced non-small cell lung cancer. *J Hematol Oncol.* 2016;9:34.

7. Xu X. Parallel phase 1 clinical trials in the US and in China accelerating the test of avitinib in lung cancer as a novel inhibitor selectively targeting mutated EGFR and overcoming T790M-induced resistance. *Clin J Cancer.* 2015;34:285-287.

8. Planken S, Behenna DC, Nair SK, Johnson TO, Nagata A, Almaden C, Bailey S, Baillard TE, Bernier L, Cheng H, Cho-Schultz S, Dalvie D, Deal JG, Dinh DC, Edwards MP, Ferre RA, Gajiwatla KS, Hemkens M, Kania RS, Kath JC, Matthews J, Murray BW, Niessen S, Orr STM, Pairsih M, Sach NW, Shen H, Shi M, Solowieij J, Tran K, Tseng E, Vicini P, Wang Y, Weinrich SL, Zhou R, Zientek, M, Liu L, Luo Y, Xin S, Zhang C, Lafontaine J. Discovery of *N*-((3*R*,4*R*)-4-fluoro-1-(6-((3-methoxy-1-methyl-1*H*-pyrazol-4-yl)amino)-9-methyl-9*H*-purin-2-yl)pyrrolidine-3-yl)acrylamide (PF-06747775) through structure-based drug design: a high affinity irreversible inhibitor targeting oncogenic EGFR mutants with selectivity over wild-type EGFR. *J Med Chem.* 2017;60:3002–3019.

9. Hao Zhang H, Wang J, Shen Y, Wang HY, Duan WM, Zhao HY, Hei, YY, Xin M, Cao YX, Zhang SQ. Discovery of 2,4,6-trisubstituted pyrido[3,4-*d*]pyrimidine derivatives as new EGFR-TKIs. *Eur J Med Chem.* 2018;148:221-237.

10. Chan BK, Hanan EJ, Bowman KK, Bryan MC, Burdick D, Chan E, Chen Y, Clausen S, Dela Vega T, Dotson J, Eigenbro C, Elliot RL, Heald RA, Jackson PS, Knight JD, La H, Lainchbury MD, Malek S, Purkey HE, Schaefer G, Schmidt S, Seward EM, Sideris S, Shao L, Wang S, Yeap SK, Yen I, Yu C, Heffron TP, Discovery of a noncovalent, mutant-selective epidermal growth factor receptor inhibitor. *J Med Chem.* 2016;59:9080–9093.

11. Uchibori K, Inasse N, Araki M, Kamada M, Sato S, Okuno Y, Fujita N, Katayama R. Brigatinib combined with anti-EGFR antibody overcomes osimertinib resistance in EGFR-mutated non-small cell lung cancer. *Nat Commun*. 2017:8:14768.

12. Jia Y, Yun CH, Park E, Ercan D, Manuai M, Juarez J, Xu C, Rhee K, Chen T, Zhang H, Palakurthi S, Jang J, Lelais G, DiDonato M, Bursulaya B, Michellys, PY, Epple, R, Marsilije, TH, McNeill M, Lu W, Harris J, Bender S, Wong KK, Janne PA, Eck MJ. Overcoming EGFR(T790M) and EGFR(C797S) resistance with mutant-selective allosteric inhibitors. *Nature* 2016;534:129-132.

13. Gűnther M, Lategahn J, Juchum M, Döring E, Keul M, Engel J, Tumbrink HL, Rauh D, Laufer S. Trisubstituted pyridinylimidazoles as potent inhibitors of the clinically resistant L858R/T790M/C797S EGFR mutant: targeting of both hydrophobic regions and the phosphate binding site. *J Med Chem.* 2017;60: 5613–5637.

14. Lu X, Zhang T, Zhu S-J, Xun Q, Tong L, Hu X, Li Y, Chan S, Su Y, Sun Y, Chen Y, Ding J, Yun C-H, Xie H, Ding K. Discovery of JND3229 as a new $EGFR^{C797S}$ mutant inhibitor with in vivo mono drug efficacy. *ACS Med.Chem.Lett*. 2018;9:1123-1127.

15. Niederst MJ, Hu H, Mulvey HE, Lockerman EL, Garcia AR, Piotrowska Z, Sequist LV, Engelman JA. The allelic context of the C797S mutation acquired upon treatment with third-generation EGFR inhibitors impacts sensitivity to subsequent treatment strategies. *Clin Cancer Res*. 2015;21:3924-3933.

16. Wang Z, Yang, JL, Huang J, Ye JY, Zhang XC, Tu HY, Han-Zhang H, Wu YL. Lung adenocarcinoma harboring EGFR T790M and in trans C797S responds to combination therapy of first- and third-generation EGFR TKIs and shifts allelic configuration at resistance. *J Thoracic Oncol*. 2017;12:1723-1727.

17. Lowder MA, Doener AE, Schepartz A. Structural differences between wild-type and double mutant EGFR modulated by third-generation kinase inhibitors. *J Am Chem Soc.* 2015;137:6456–6459.

18. Gangemi S, Franchina T, Mincuillo PL, Profita M, Zanghi M, David A, Kennez I, Adamo, V. IL-33/IL-31 axis: a new pathological mechanism for EGFR tyrosine kinase inhibitors-associated skin toxicity. *J Cell Biochem*. 2013;114: 2673-2676.

19. Tsou HR, Overbeek-Klempers EG, Hallet WA, Reich MF, Floyd MB, Johnson BD, Michalak RS, Nilakantan R, Discafani C, Golas J, Rabindran SK, Shen R, Shi X, Wang YF, Upeslacis J, Wissner, A. Optimization of 6,7-disubstitiuted-4-(arylamino)quinolone-3-carbonitriles as orally active, irreversible inhibitors of human epidermal growth factor receptor-2 kinase activity. *J Med Chem*. 2005;48: 1107-1131.

20. Jester BW, Cox KJ, Gaj A, Shomin CD, Porter JR, Ghosh I. A coiled-coil enabled split-luciferase three-hybrid system: applied toward profiling inhibitors of protein kinases. *J Am Chem Soc.* 2010;132:11727-11735.

21. Karaman MW, Herrgard S, Triber DK, Gallant P, Atteridge CE, Campbell, BT, Chan KW, Ciceri P, Davis MI, Edeen PL, Faraoni R, Floyd M, Hunt JP, Lockhart DJ, Milanov ZV, Morrison MJ, Pallares G, Patel HK, Pritchard S, Woodicka LM, Zarrinkar PA. Quantitative analysis of kinase inhibitor selectivity. *Nat Biotechnol.* 2008;26:127–132.

22. Zhang WJ, Wei H' Hagen T' Frei, B. α-Lipoic acid attenuates LPS-induced inflammatory responses by activating the phosphoinositide 3-kinase/Akt signaling pathway. *Proc Natl Acad Sci. U.S.A*. 2007;104:4077-4082

23. Antonello A, Tarozzi A, Morroni F, Cavalli A, Rosini M, Hrelia P, Bolognesi ML, Melchiorre C. Multi-target directed drug design strategy: a novel molecule designed to block epidermal growth factor receptor (EGFR) and to exert proapoptotic effects. *J Med Chem*. 2006;49:6642-6645.

24. Beno BR, Yeung, K-S, Bartberger, MD, Pennington, LD, Meanwell, NA. A survey of the role of noncovalent sulfur interactions in drug design. *J Med Chem*. 2015;58:4383-4438.

25. For role of 1,2-dithiolane derivatives in DNA damage, see Nejad MI, Yang D, Shen B, Gates KS. Oxidative activation of leinamycin E1 triggers alkylation of guanine residues in double-stranded DNA. *Chem Commun*. 2018;54:256-259.

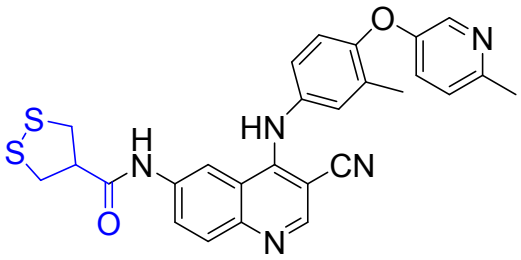

14

IC_{50} (nM)
$EGFR^{L858R}$ >10,000

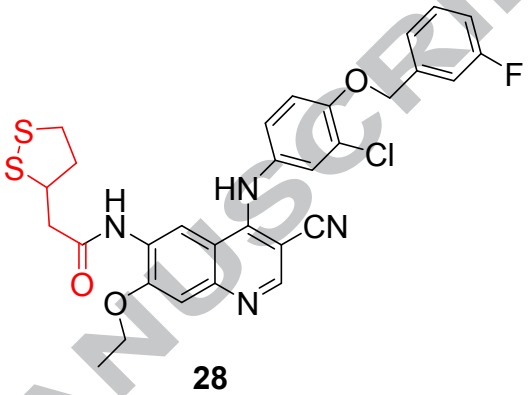

28

	IC_{50} (nM)		Kd (nM)
$EGFR^{L858R}$	11	$EGFR^{ex19del}$	48
$EGFR^{WT}$	120	$EGFR^{L861Q}$	4.8
$EGFR^{Her2}$	160	$EGFR^{719C}$	5.7

FIGURE LEGENDS

Figure 1. Key Aniline Intermediates 1-8

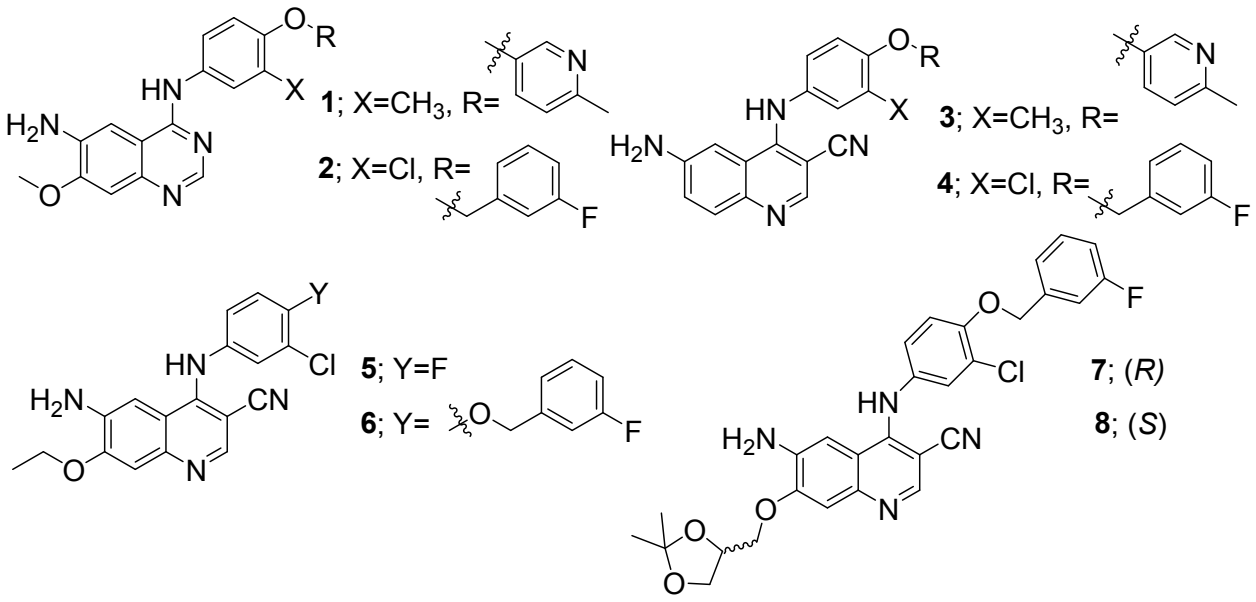

Figure 1. Key Aniline Intermediates **1-8**.

SCHEMES LEGENDS

Scheme 1. Synthesis Protocol for 7 and 8.

Scheme 2. Synthesis of TKIs by Methods A, B and C

Scheme 3. Synthesis of 29-32

Scheme 1. Synthesis Protocol for 7 and 8

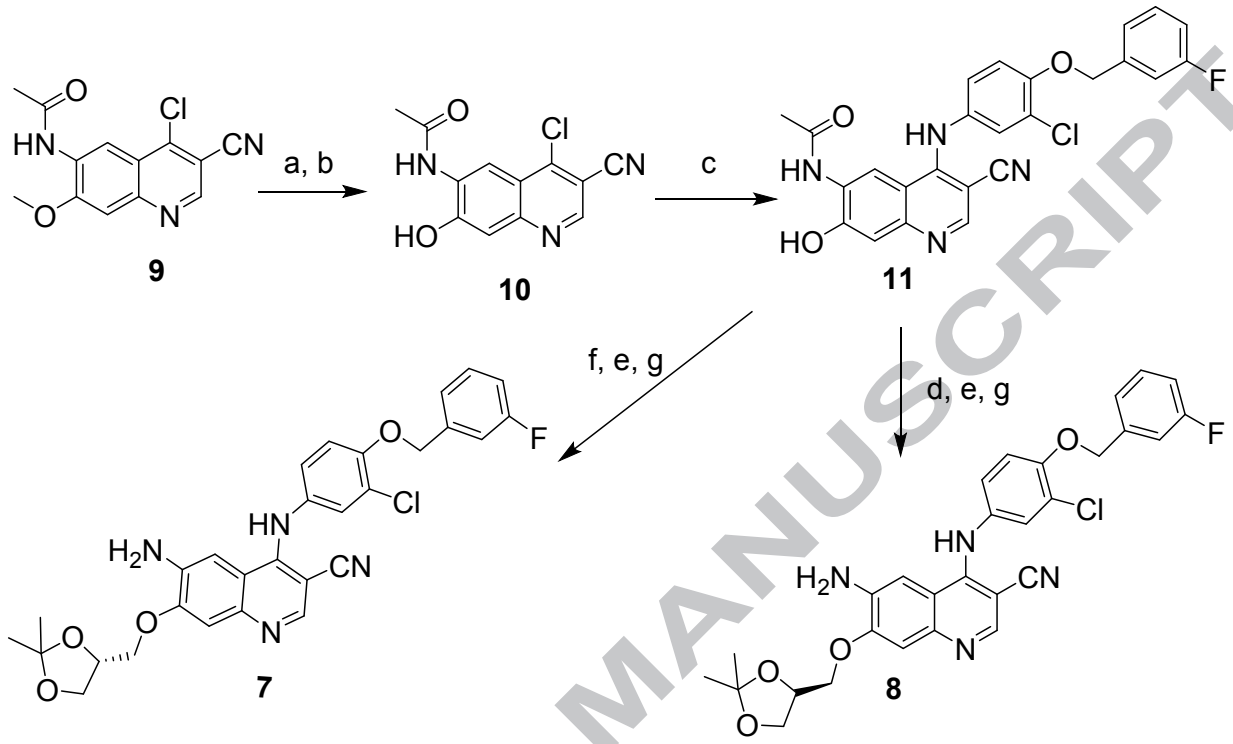

Reagents and conditions: (a) BBr_3 DCM, 0 ^oC 0.5 h, (b) 100 ^oC, 5 h, 80% , (c) 3-chloro-4-((3-fluorobenzyl)oxy) aniline, *i*-propanol, 150 ^oC 12 h 56%, (d) Cs_2CO_3 DMF, rt 0.5 , (e) *(R)*-(2,2-dimethyl-1,3-dioxolan-4-yl)methyl methanesulfonate 90 ^oC, 12 h, 12%, (f) *(S)*-(2,2-dimethyl-1,3-dioxolan-4-yl)methyl methanesulfonate 90 ^oC, 12 h, 12%, (g) KOH/MeOH 70 ^oC 6 h, 25%

Scheme 2. Synthesis of TKIs by Methods A, B and C

Method A

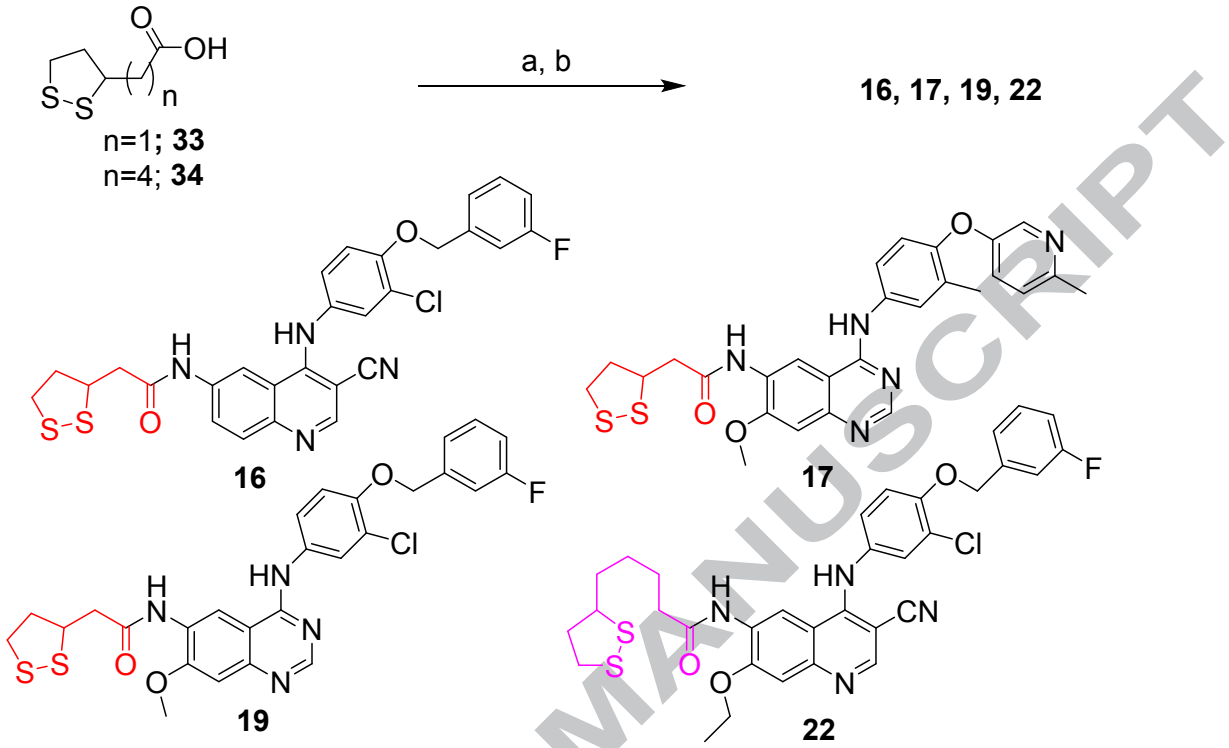

Reagents and conditions: (a) Oxalyl chloride, DCM-THF 0 ^{o}C, 15 min, (b) Anilines **1, 2, 4, 6,** DIEA, DMF-THF 0 ^{o}C, 1 h, 8-13% 2 steps.

Method B

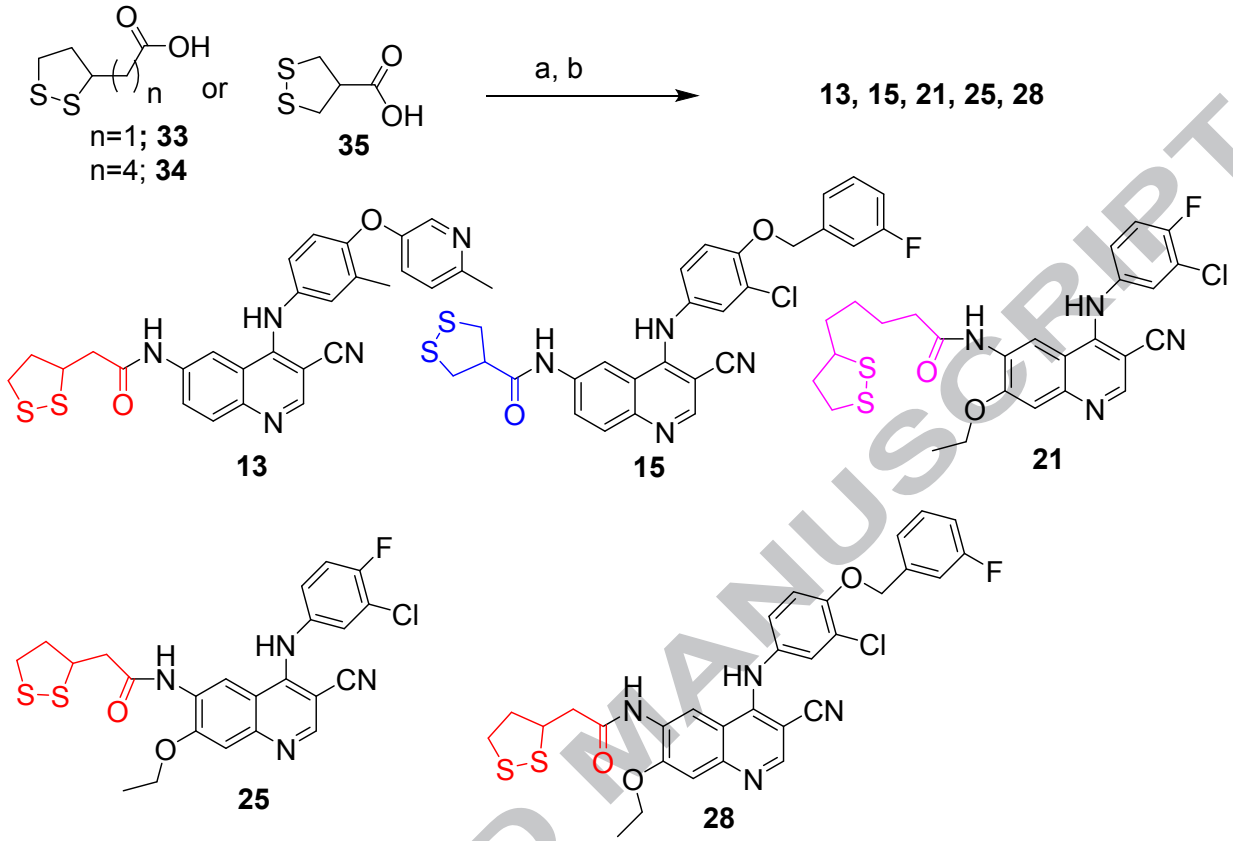

Reagents and Conditions: (a) EDC, NMP (b) Anilines **3, 5, 6** rt 2 h, 17-37% 2 steps

Method C

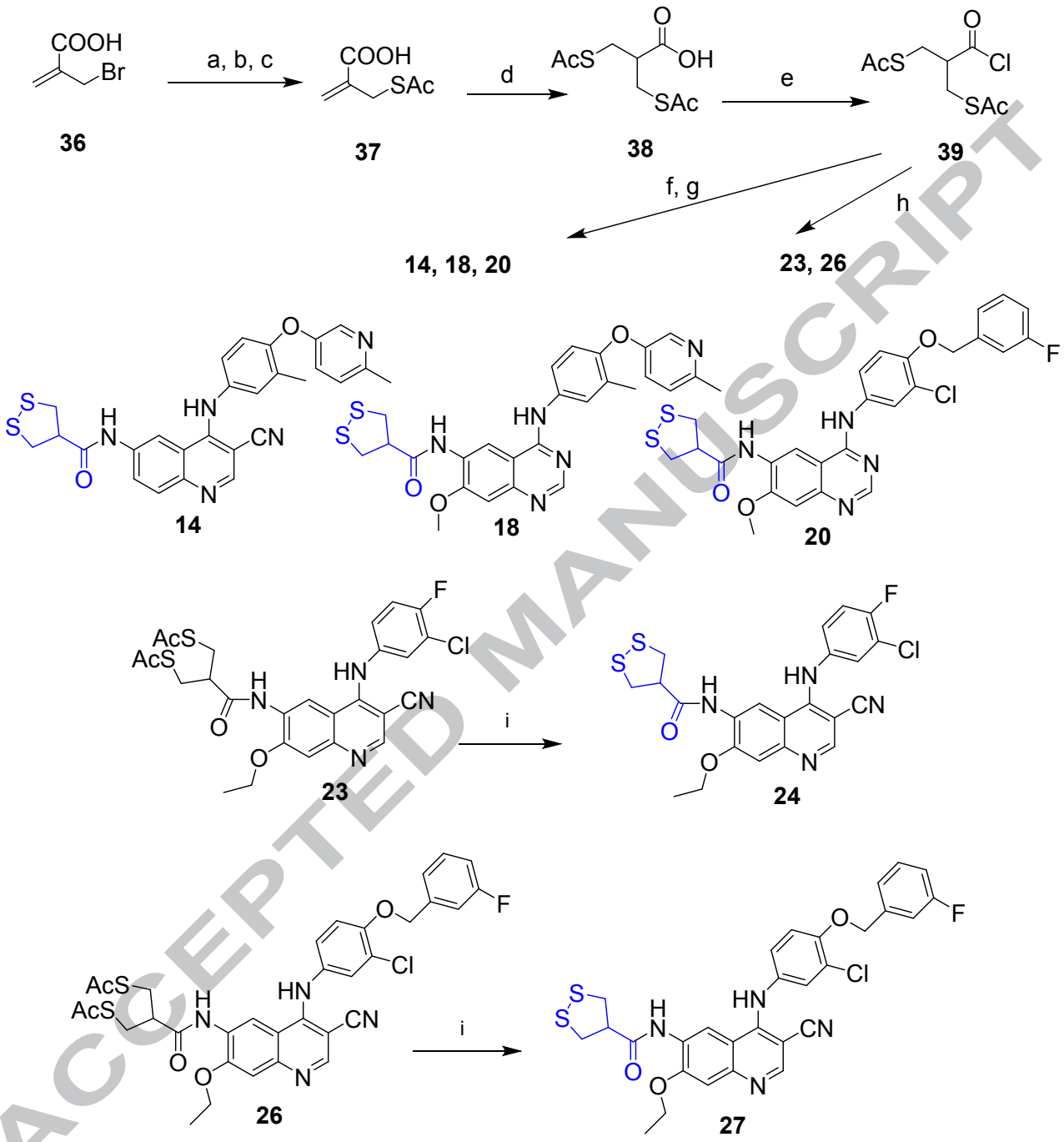

Reagents and conditions: (a) Na_2CO_3-H_2O 47% (b) AcSH (c) HCl 45% (d) AcSH 45% (e) Oxalyl chloride DCM-THF, DIEA 0 ^oC, 1 h, (f) anilines **1, 2, 3** (g) NH_3 in MeOH 2-4% 3 steps from **38** (h) anilines **5**, **6** 4% (i) **23** to **24** and **26** to **27** $NaBH_4$ DMA (i) DMSO 120 ^oC, 1 h, 12-17% 2 steps

Scheme 3. Synthesis of 29-32

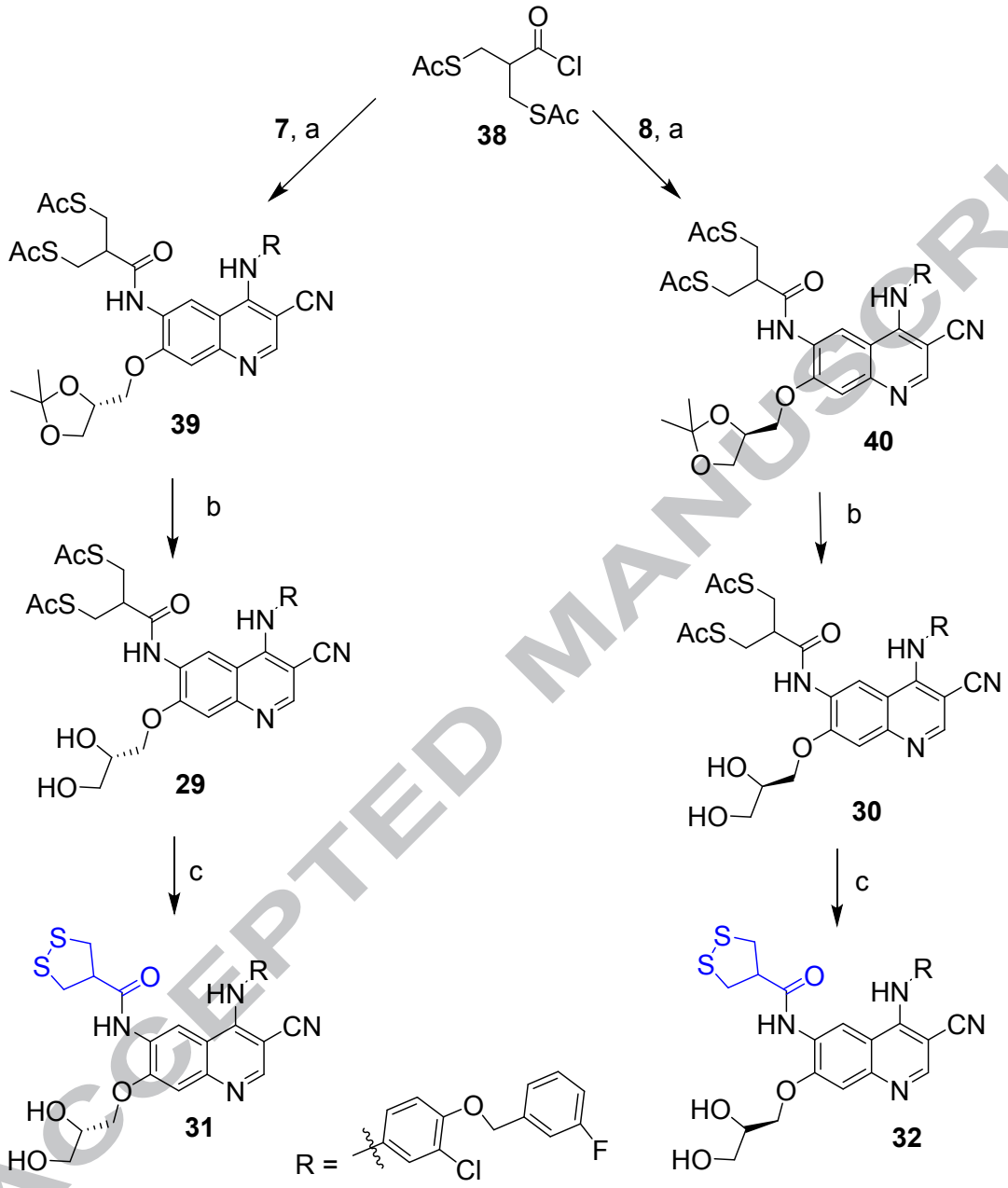

Reagents and conditions: (a) Method C DIPEA-DCM, rt 2 h, 34-63% (b) HCl MeOH rt 30 min, 10% (c) NH_3 MeOH rt 30 min, 75%

TABLE LEGENDS

Table 1. SAR in Rabbit Reticulocyte Assay (IC_{50} Values in nM)

Table 2. IC_{50} Values (nM) Against Her2 in the Rabbit Reticulocyte Lysate Assay

Table 3. Cellular Activity in μM of 17 and 28 in the NCI-60 Panel

Table 1. SAR in Rabbit Reticulocyte Assay (IC_{50} Values in nM)*

Entry	Compound	$EGFR^{WT}$	$EGFR^{L858R}$	Method
1	**13**	8630 ± 850	>10,000	B
2	**14**	>10,000	>10,000	C
3	**15**	NT	199 ± 19	B
4	**16**	164 ± 15	36 ± 12	A
5	**17**	253 ± 20	48 ± 8	A
6	**18**	658 ± 219	413 ± 68	C
7	**19**	25 ± 2	5.8 ±1	A
8	**20**	76 ± 6	6.5 ± 0.8	C
9	**21**	NT	420 ± 5	B
10	**22**	730 ± 65	33 ± 4	A
11	**23**	NT	494 ± 30	C
12	**24**	NT	219 ± 47	C
13	**25**	NT	300 ± 40	B
14	**26**	340 ± 67	26.8 ± 4.2	C
15	**27**	210 ± 20	18 ± 3	C
16	**28**	120 ± 19	10.9 ± 1.9	B
17	**31**	125 ± 12	9 ± 2	C
18	**32**	256 ± 21	20 ± 7	C

*Ten point dose response curve, each value is an average of triplicate experiments

Table 2. IC_{50}* Values (nM) against Her2

Entry	Compound	$EGFR^{WT}$	$EGFR^{L858R}$	Her2
1	**13**	8630 ± 850	>10,000	>10,000
2	**16**	164 ± 15	36 ± 12	730 ± 150
3	**17**	253 ± 20	48 ± 8	93 ± 19
4	**18**	658 ± 219	413 ± 68	590 ± 155
5	**27**	210 ± 20	18 ± 3	730 ± 150
6	**28**	120 ± 19	10.9 ± 1.9	160 ± 20
7	**31**	125 ± 12	9 ± 2	167 ± 20

*Ten point dose response curve, each value is an average of triplicate experiments

Table 3. Cellular Activity in μM of 17, 28 and Gefitinib in Select Cells in the NCI-60 Panel[a]

	17			28			Gefitinib
Cell Line	GI_{50}[b]	LC_{50}[c]	TI[d]	GI_{50}[b]	LC_{50}[c]	TI[d]	GI_{50}[e]
NSCLC							
A549	0.76	NT		0.54	3.4	6.2	7.94
NCI-H322M	1.07	> 50	> 46.7	0.60	> 25	> 41.5	0.08
NCI-H460	0.11	NT		0.47	1.95	4.1	6.31
Leukemia							
CCRF-CEM	0.22	> 50	> 227	0.15	> 25	> 166	5.01
MOLT-4	0.16	> 2.6	16.2	0.16	> 25	> 156	3.98

(a) Five dose response curve, each value is an average of 2 experiments; (b) GI_{50} is the concentration of the drug causing 50% growth inhibition (c) LC_{50} is the cytotoxic concentration due to 50% reduction in measured protein (d) LC_{50}/GI_{50} (e) data from the DTP-NCI database https://dtp.cancer.gov/services/nci60data/meangraph/gi50/jpg/-4.0/715055